ACTA STEREOL 1984; 3/2: 113-138
REVIEW ARTICLE

BASIC CONSIDERATIONS FOR MEASURING IN IMAGES

Dieter Vollath

Kernforschungszentrum Karlsruhe GmbH
Institut für Material- und Festkörper-
forschung III, Postfach 3640
D-7500 Karlsruhe (Federal Republic of Germany)

ABSTRACT

Before any measurements can be carried out in an image, it must first be clarified how such dimensions are brought about. It is explained that dimensions most likely to be used such as areas, perimeters and Euler numbers, must be defined in such a way that no conflicts in logic can arise. This paper explains basic considerations which have to be made prior to any measurement and the consequences of tessellating the Euclidean plane.

0. INTRODUCTION

All the theories and formulae in stereology are based on the Euclidean metric. If we analyse images using computers we have to discretize the plane of the image. In this tessellated plane the Euclidean metric is no longer valid. So we have to analyse the consequences of tessellating the plane for measurements with computers and to find possibilities of using all the formulae developed for the Euclidean plane as an approximation. This paper aims at explaining how measured values can be obtained in a tessellated plane such that no conflict in logic can arise. It is not intended to present a complete review of the literature and of the state of the art in this field. The idea is rather to give an introduction to those readers not familiar with the problems in question.

1. MEASURING GRID

When processing images we will limit ourselves initially

to images situated in one plane. This plane represents a continuous two - dimensional space in which Euclidean metrics applies ($\mathbb{R}^2$). The images are digitized by superimposing a measuring grid and determining the brightness (the functional value) of the image at the different grid points. In physical terms, the digitized value now represents the average of the brightness distribution around such a grid point. The grids normally used are regular subdivisions of the plane by means of polygons. If it is to be assured that each point in the plane is considered precisely once, the environments around the different grid points must be chosen so as to result in complete tessellation of the plane. The transition from an image in the object space to an image stored in the computer is a transformation from a Euclidean space into a discrete space.

If the plane is to be tessellated completely with regular polygons of n sides, the number of polygons of n sides meeting at each corner will be (Coxeter, 1963)

$$m = \frac{2n}{n-2} \qquad (1)$$

In the centers of these polygons with n sides (unit cells) are the grid points to which the readings are assigned. If these unit cells constitute polygons with n sides, the grid points are arranged in the form of regular polygons of m sides. It is easy to see that only the three following integer relationships between m and n exist for Equation (1):

m	3	4	6
n	6	4	3

Coxeter (1963) has shown this to be the only possibility of tessellating the plane with regular polygons of n sides. These measuring grids will be briefly explained below. Figs. 1a, b, c shown the grids.

The simplest measuring grid is the Cartesian grid, m = 4, n = 4 (Fig. 1a). In this case, all grid points are points of $\mathbb{Z}^2$. The functional value to be assigned to a grid point represents the mean of the functional values within a unit cell which, in this case, is square. In a similar way, a hexagonal grid (m = 6, n = 3) (Fig. 1b) can be defined, in which each functional value to be assigned to each individual grid point is the mean of the hexagon

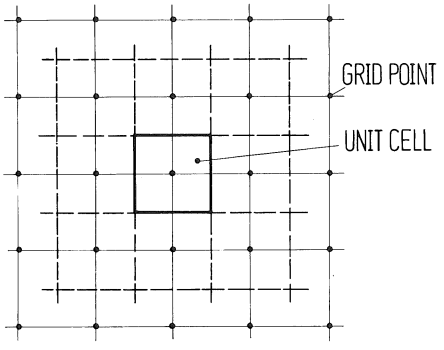

Fig. 1a:

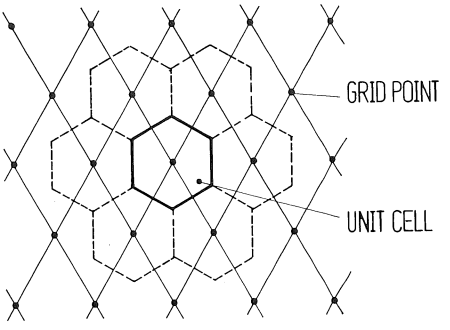

Fig. 1b:

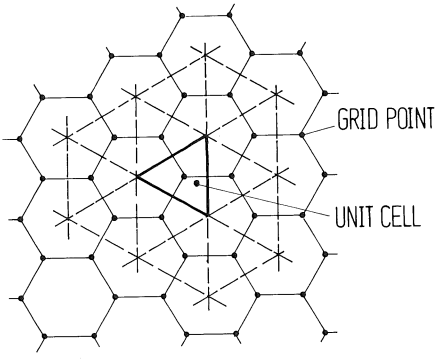

Fig. 1c:

Fig. 1a: Arrays of unit cells and grid points in a Cartesian system of coordinates.

Fig. 1b: Arrays of unit cells and grid points in a system of hexagonal coordinates.

Fig. 1c: Arrays of unit cells and grid points in a system of triangular coordinates.

surrounding that grid point. The grid points proper are arranged as equilateral triangles. Finally, there is tessellating of the plane with triangles (m = 3, n = 6), the triangular grid (Fig. 1c). In this grid, the functional value to be assigned to a grid point is the mean within the triangle surrounding the grid point. However, this grid is not used for practical purposes (Gray, 1971; Peipmann, 1976).

2. CONNECTIVITIES OF ADJACENT POINTS

Let us consider two points, p_i (x_i, y_i) and p_j (x_j, y_j), and the sets $P_i = \{p_i\}$ and $P_j = \{p_j\}$, containing these points. In this way, we can define a neighborhood around a point by defining the connectivity of two points by means of a small set, S, describing the neighborhood of the origin. Two points, p_i and p_j, are adjacent, if

$$P_i \cap (P_j \oplus S) \neq \emptyset \;.\wedge.\; P_j \cap (P_i \oplus S) \neq \emptyset \quad i \neq J \qquad (2a)$$

For

$$P_i \cap (P_j \oplus S) = \emptyset \ .v. \ P_j \cap (P_i \oplus S) = \emptyset \qquad i \neq j \qquad (2b)$$

$\oplus$ stands for the Minkowski addition (dilation) (Hadwiger 1950, Matheron 1967)

the points, p_i and p_j, are not adjacent. In the Euclidean plane, two points are called adjacent, if

$$p_i \in U(p_j)$$
$$U(p_j) = \left\{ p_i \in \mathbb{R}^2 \,|\, d(p_i, p_j) < \varepsilon \right\} \qquad (3)$$

where $d(p_i, p_j)$ is the Euclidean distance between the points p_i and p_j, and ε is correspondingly small. This definition is a special case of definition (2) for a circular set, S. Definition (2) has the advantage over (3) of being restricted neither to Euclidean space, nor to an isotropic neighborhood. In a discrete space, each point has only a finite number of neighbors (connectivities). In principle, there may be freedom in choosing these connectivities, but any choice of connectivities has far reaching impacts on the representation and the measurement of shapes in a geometry defined in this way.

In the case of a discrete space, the set S, describing the neighborhood of a point consists of the origin and the points meant to be adjacent to it. To be meaningful, it must contain at least one additional grid point besides the origin.

2.1 CARTESIAN COORDINATES

Fig. 2 shows the eight possible neighbors of an image point with the coordinates (i, j). Obviously, the four immediately adjacent unit cells with the coordinates (i, j - 1), (i, j + 1), (i - 1, j) and (i + 1, j) must be regarded as neighbors. However, in this case of application these four neighborhoods are not enough. If we consider the image of a straight line in Euclidean space in the existing discrete space we see that, for such a straight line, there exist only two directions located normal to each other in which a straight line is also represented as a "straight line." In all directions not parallel to the coordinate axes, a straight line imaged in discrete space breaks down into "line segments" or points.

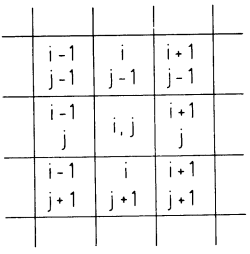

Fig. 2: Counting unit cells in a system of Cartesian coordinates.

If also the diagonal unit cells with the coordinates (i - 1, j - 1), (i - 1, j + 1), (i + 1, j - 1) and (i + 1, j + 1) are regarded as being adjacent, each straight line in the Euclidean plane will also be imaged on a closed traverse line. In discrete space, a traverse line is supposed to be an ordered set of points in which each point, p_j, has not more than two neighbors, p_{j-1} and p_{j+1}, which are adjacent to the point, p_j, for the definition selected for connectivity. If each point has precisely two neighbors, it is a closed traverse line. The assumption of eight possible neighbors (connectivities) in the Cartesian system is the assumption used most frequently (Rosenfeld, 1966, 1970). Below, only the case involving eight connectivities of a point will be considered. The set, S, describing the neighborhood of the origin therefore consists of the origin and the eight points surrounding it.

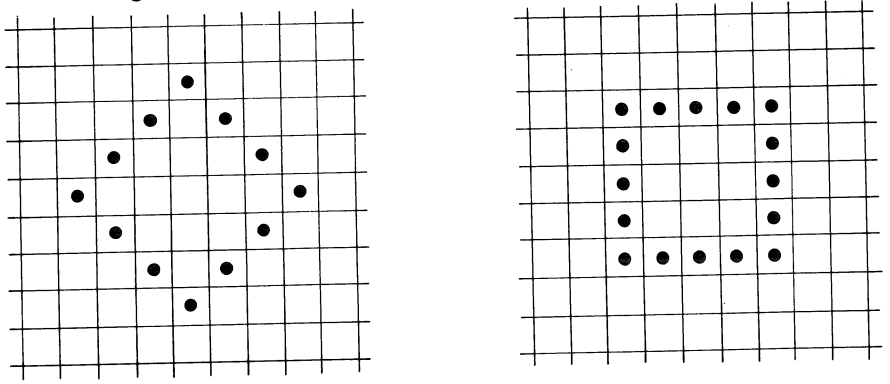

Fig. 3: Curve in a system of Cartesian coordinates producing connected and unconnected sets.

Inclusion of the unit cells connected by way of the diagonals results in the interesting paradox which makes it possible to have a closed traverse line not producing two disjunct sets. Fig. 3a, b show the contours of two squares. While, in the square shown in Fig. 3a, the inside and the outside are disjunct and not connected, this is not true of the square in Fig. 3b, which is shown turned around by 45 degrees. In the square shown in Fig. 3b, only the connectivities trough the directions of the diagonals were used. If a connection between the unit cells (i, j) and (i + 1, j + 1) is assumed (covered points), it is obvious that also the unit cells (i + 1, j) and

(i, j + 1) are connected. Hence, that area of the plane, which is surrounded by the square standing on its tip in Fig. 3b, is not separated from the remainder of the plane. Unlike Fig. 3a, the closed curve shown in Fig. 3b is not a Jordan-type curve. Rosenfeld (1966, 1970) has drawn attention to this paradox.

The Japanese game of GO makes use of the very fact that in a discrete Cartesian system a closed curve is not in every case also a Jordan-type curve.

2.2 HEXAGONAL COORDINATES

Fig. 4 shows the unit cells in a hexagonal grid. It is clearly seen that there is only one type of neighboring elements. There are no unit cells meeting only in one point. Consequently, connectivities cannot intersect. For this reason, every closed curve in this hexagonal system is also a Jordan-type curve.

2.3 PARTICLE CONNECTIVITY

Some properties of binary images will be examined below. Let an image be the subset $B(x, y) \subset \mathbb{R}^2$ or, in case of a discrete space, $B(m, n) \subset \mathbb{Z}^2$, in which N particles are contained which can be individualized. The set, B (x, y), can be broken down into N paired disjunct nonempty subsets (particles), G_i (x, y), (in case of a discrete space, G_i (m, n)).

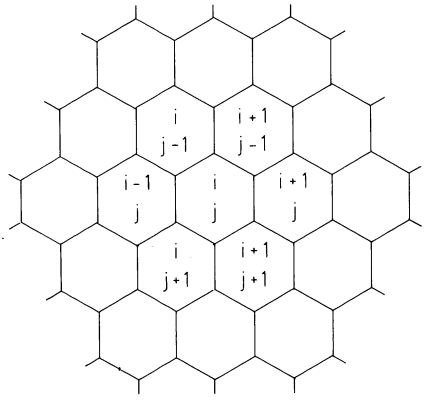

Fig. 4: Counting unit cells in a system of hexagonal coordinates.

$$B = \bigcup_{i \in I} G_i \qquad I = \{1, 2 \ldots N\}$$

$$G_i \cap G_j = \emptyset \qquad i \neq j$$

On the basis of definition (2), let two subsets, G_i and G_j $(i \neq j)$, be disjunct and not connected, if

$$G_i \cap (G_j \oplus S) = \emptyset \;.\wedge.\; G_j \cap (G_i \oplus S) = \emptyset \qquad (4)$$

As in 2., S defines the neighborhood of a point. In addition, we can also indicate a boundary C_i (G_i), for each particle.

If (4) is met, we will construct a boundary C_i (G_i), for which it holds that

$$C_i\ (G_i) \cap C_j\ (G_j) = \emptyset \tag{5}$$

because the subsets are not connected. Condition (5) is met, if

$$C_i\ (G_i) \subset (G_i \oplus S) \tag{6}$$

Hence, for reasons of better clarity, the subsets G_i, are frequently regarded as being closed i.e., $C_i \subset G_i$ (Peipmann, 1976). We will have to examine whether this assumption meets all criteria.

If we consider two sets located at the smallest possible distance from each other, it holds that

$$(G_i \oplus S) \cap (G_j \oplus S) \neq \emptyset \tag{7}$$

We will now find the largest set, $S' \subset S$, which, in this case, meets the condition of

$$(G_i \oplus S') \cap (G_j \oplus S') = \emptyset \tag{8}$$

Condition (8) can only be met for a pair of sets, G_i and G_j, if $S' \cap \tilde{S}' = \{0\}$, where $\tilde{S}'$ is produced by mirroring S' from the origin. The set $\{0\}$ contains only the origin. In order to prove that this condition is not sufficient, let us look at the example of a dilation of two parallel straight lines, g, which are parallel to $\vec{e}_1$ at the distance of two image points:

$$\vec{g}_1 = \vec{a}_1 + \lambda\ \vec{e}_1$$
$$\vec{g}_2 = \vec{a}_1 + 2\ \vec{e}_2 + \lambda\ \vec{e}_1$$

These straight lines are dilated by means of vectors, $\vec{n}_1 = \alpha_1\ \vec{e}_1 + \alpha_2\ \vec{e}_2$ and $\vec{n}_2 = \beta_1\ \vec{e}_1 + \beta_2\ \vec{e}_2$ $\alpha_i, \beta_i \in \{-1,0,1\}$ from the set of local vectors describing the points of S. The straight lines $\vec{g}_i'$, produced by dilation (border line of $\vec{g}_1 \oplus \vec{n}_i$) are

$$\vec{g}_1 = \vec{a}_1 + \lambda\ \vec{e}_1 + \alpha_1\ \vec{e}_1 + \alpha_2\ \vec{e}_2$$
$$\vec{g}_2 = \vec{a}_1 + \lambda\ \vec{e}_1 + 2\ \vec{e}_2 + \beta_1\ \vec{e}_1 + \beta_2\ \vec{e}_2$$

These two new straight lines coincide if and only if

$$\alpha_2 = 2 + \beta_2$$

Because of the range of values of α_i and β_i, this condition is met whenever $\alpha_2 = -\beta_2$. An essentially equivalent result is obtained by turning the straight lines around.

This means that we obtain for S'

$$S' = \bigcup_{i \in I} p_i \ (a, b) \qquad I = \{1, 2 \ldots\ldots 8\} \tag{9}$$

where p_i are the local vectors describing the neighboring points of the origin.

$$\vec{p}_i = a_i \vec{e}_1 + b_i \vec{e}_2$$

For the coefficients, a_i and b_i, it then holds that

$$\left(\forall i{:}a_i \in \{0, 1\}\right) \nabla \left(\forall i{:}a_i \in \{-1, 0\}\right) \qquad i \in \{1,\ldots,8\}$$
$$\left(\forall i{:}b_j \in \{0, 1\}\right) \nabla \left(\forall i{:}b_j \in \{-1, 0\}\right)$$

∇ stands for the exclusive or connection.

Since (5) applies at the same time, it holds that

$$G_i \oplus S' \subseteq G_i \cup C_i \ (G_i)$$

Coefficients of measure must be found to characterize images in quantitative terms (such as samples of materials). When surveying images B it is generally necessary to decompose into M subfields, B_1, the field, F, to be surveyed of the image, B. For this to be permissible, only those measures $\mu\ (B_1)$ may be determined for which

$$\sum_{1 \in L} \mu\ (B_1) = \mu\ \Big(\bigcup_{1 \in L} B_1\Big) \qquad L = \{1,2, \ldots M\}$$

This applies correspondingly also to all G_i

$$\sum_{i \in I} \mu\ (G_i) = \mu\ \Big(\bigcup_{i \in I} G_i\Big), \qquad I = \{1, 2, \ldots N\} \tag{10}$$

This means that we only consider those measures, μ, which are σ-additive. Gray (1971) has shown this to be true for the areas, the perimeter and the Euler number. This is also evident in the light of conditions (4) and (5). While the areas and the perimeter are positive and monotonic measures to which

$$\mu(G_i) > 0, \quad \mu(B_1) > 0$$

and $$\mu(G_i) < \mu(B_1) \text{ for } G_i \subset B_1$$

and $$\mu(B_1) < \mu(B) \text{ for } B_1 \subset B$$

respectively, apply, this is generally not true of the Euler number.

Because of the additivity of the three measures considered above, it holds for our image, B, that

$$\mu(B) = \mu\left(\bigcup_{i \in I} G_i\right) = \sum_{i \in I} \mu(G_i) \quad I = \{1, 2, \ldots N\} \qquad (11)$$

Under conditions (4) and (5) it is irrelevant whether the individual particles (= subsets) of an image are individualized or not before determining the coefficient of measure.

3. MEASURES AND METRICS

3.1 DEFINITIONS OF AREAS AND PERIMETERS

Only the areas of particles and their perimeters are to be studied as measures below, because only they are bound to metrics. This requires the following definitions to be agreed upon:

In a system of particles $\bigcup_{i \in I} G_i = B \subset \mathbb{R}^2$

the following relations apply between the definitions of the connectivity of subsets G_i (Eq. 4), the rule defined therein for a boundary, C_i, (Eq. 5) and the measures for the area, A, and the perimeter, P, of these subsets:

$$\oint_{C_i} ds = P \qquad (12)$$

$$\frac{1}{2} \oint_{C_i} (x\,y' - y\,x')\,ds = A \qquad (13)$$

The integration path, C_i represents a boundary of G_i according to Eq. (5).

As performed in $\mathbb{R}^2$ in this case, a system supposed to be consistent in a discrete space must obey the criterion of allowing a contour to be defined through the definition of neighborhoods (connectivities) in such a way that this contour can be used as an integration path to measure the area and the perimeter, taking into account a metric adequate to the grid. With the metrics of discrete space taken into account, the elementary geometric relationships must apply between the perimeter and the area.

If one changes to a discrete space, one considers the quantity, B (m, n), containing the particles, G_i (m, n),

$$G_i \subset B$$

The particle, G_i, by definition has the area of

$$A(G_i) = \sum_{m,n} I_{G_i} \quad (m, n) \quad m, n \in \{1, 2 \ldots N\} \qquad (14)$$

I_{G_i} (m, n) being the indicator function of G_i. This formula implies that the number of discrete points making up G_i is taken as an area. Moreover, we want to consider boundaries, C_i (G_i), meeting criteria (5) and (6). A boundary, C_i, represents a closed line. If a parameter description, $C_i = C_i$ (1) $1 \in \{1, 2 \ldots L_i\}$, is chosen for C_i (m, n), L_i is the length of the traverse line (= number of grid points making up C_i). Writing down formulae (12) and (13) for a discrete space by analogy provides

$$M_i = \sum_{1 \in L} I_{C_i}(1) \qquad L = \{1, 2 \ldots M_i\} \qquad (15)$$

$$N_i = \sum_{1 \in L} \left\{ m(1) \cdot [n(1+1) - n(1)] - n(1)[m(1+1) - m(1)] \right\} \qquad (16)$$

If the result, N_i, is in accordance with the area defined in Eq. (14) and if conditions (5) and (6) for a boundary have been met in setting up C_i, the result, M_i, is the perimeter

of G_i. Of course, this implies that the boundary, C_i, has been chosen so as to meet the conectivity conditions of the underlying space. This also applies to the interpretation of the coefficient of measure of the perimeter.

In all systems meeting criteria (4, 5, 6, 14, 15) and (16) it is irrelevant whether the measurements are carried out by counting points (if necessary, after the appropriate transformations) or by tracing contours. The criterion of the measurements of the area and the perimeter being conducted on a uniform basis also in $\mathbb{Z}^2$ becomes more important, especially, when the area and the perimeter are measured in a sample and conclusions with respect to possible shapes are drawn from their relationship.

For length measurements in $\mathbb{R}^2$ and $\mathbb{Z}^2$ we use the Minkowski measure for the distance between points p_i and p_j:

$$d\,[p_i(x_i,y_i),p_j(x_j,y_j)]=\left(|x_i-x_j|^n+|y_i-y_j|^n\right)^{1/n} \qquad (17)$$

where, in $\mathbb{R}^2$, n = 2 (Euclidean distance) and, in discrete Cartesian space, $\mathbb{Z}^2$, n = 1 (taxi metrics) is used.

In case of hexagonal tessellation of the plane, the hexagonal distance function indicated by Rosenfeld, Pfaltz (1968) must be applied:

$$d\left[p_i\,(x_i,\,y_i),\,p_j\,(x_j,\,y_j)\right] =$$

$$= \text{Max}\left(|x_i-x_j|,\frac{1}{2}\left(|x_i-x_j|+(x_i-x_j)\right)-\left(\left\lfloor\frac{x_i}{2}\right\rfloor-\left\lfloor\frac{x_j}{2}\right\rfloor\right)+y_j-y_i,\right.$$

$$\left.\frac{1}{2}\left(|x_i-x_j|-(x_i-x_j)\right)+\left(\left\lfloor\frac{x_i}{2}\right\rfloor-\left\lfloor\frac{x_j}{2}\right\rfloor\right)+y_i-y_j\right)$$

$$x_i,\ y_i \in \mathbb{Z}$$

$\lfloor x_i \rfloor$ is the largest integer not exceeding x_i. As has been shown by Rosenfeld and Pfaltz, this distance function meets all criteria of a metric in a hexagonally tesselated plane.

3.2 PERFORMING MEASUREMENTS IN CARTESIAN COORDINATES

According to the definition of the neighborhood of a point indicated in 2. the quantity S describing the neighborhood of a point has the appearance shown in Fig. 5.

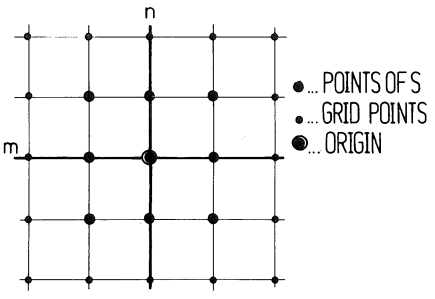

Fig. 5: Set S describing the neighborhood of a point in the system of Cartesian coordinates.

Fig. 6 shows a set, P_1, and its neighborhood $P_1 \oplus S$, and three additional disjunct sets located at the shortest possible distance from P_1. Now a contour, C, can be defined, which meets criterion (5) and in which the result obtained from (16) is equal to the area to be determined by counting. This contour is obtained by assigning an area of 1 to each unit cell in accordance with (14) and tracing the outer boundary of the unit cells of a figure. If the unit cells are shifted in such a way that one corner point each lies on a grid point, this contour can be described by a sequence of grid points. Consequently, the contour, C, is determined by

$$C = (B \oplus S') \cap (\overline{B} \oplus S')$$

The set, S', has been plotted in Fig. 7. Besides the set, S', indicated, the sets originating from turning S' around the origin in 90^o steps furnish contours with the same properties, because all four corners of the unit cell can be moved into the grid point. Obviously, the contour forming set, S', must be a subset of the set, S, defining the neighborhood, because otherwise criterion (5) cannot be met.

The perimeter measurable in accordance with (12) indicates the perimeter in taxi metrics, for also in calculating the area, the integration path, C, must be covered in the sense of taxi metrics. Since $\tilde{S}' \cap S' = \{0\}$ and also criterion (9) is met, also criterion (5) will be met in every case. From the definition (19) of the boundary it is apparent that the subsets, G_i, must not be regarded as closed.

Fig. 8 shows the same arrangement of sets as Fig. 6, but the sets $P_1,\ldots,P_4$ are also shown with their contours $C_1,\ldots,C_4$.

As can be seen from Fig. 8, the contour determined in accordance with Eq. (19) is a Jordan-type curve. It is also interesting to point out that $S' \oplus \tilde{S}' = S$.

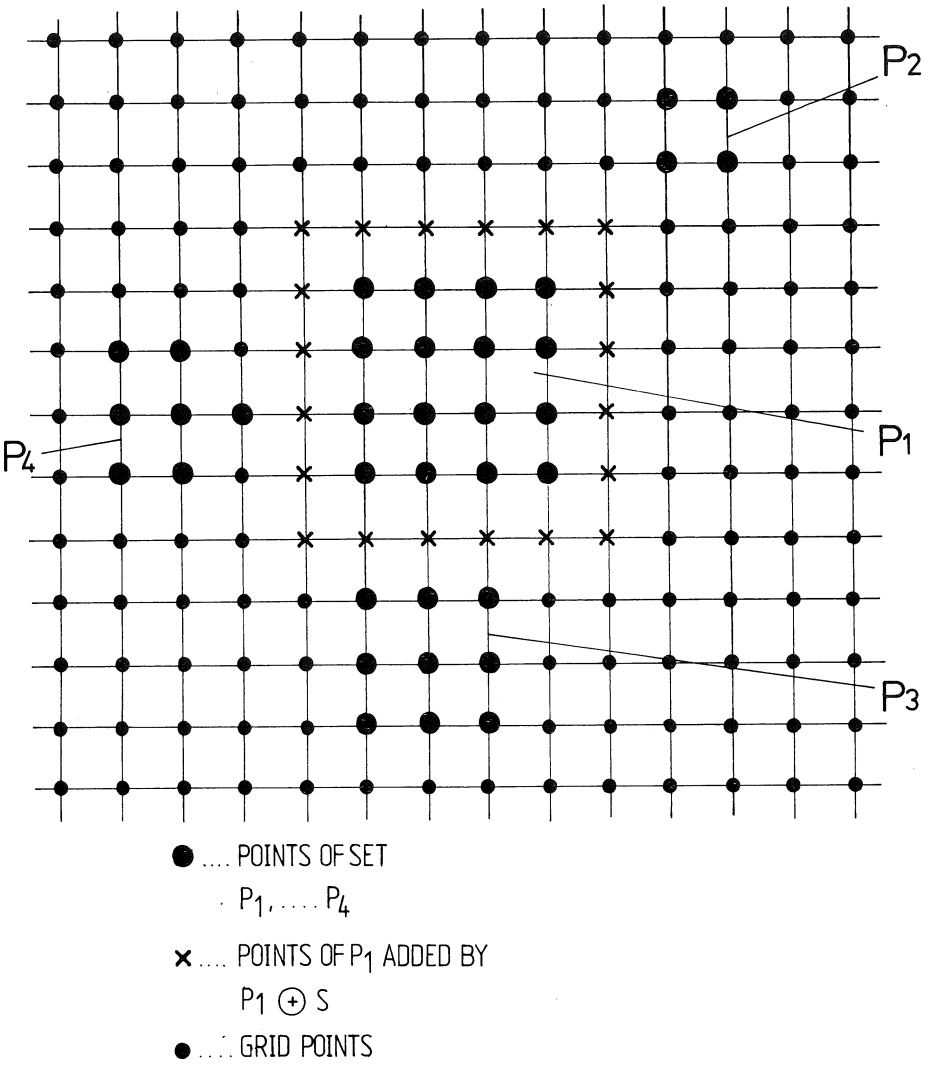

Fig. 6: Neighborhood of the set, P_1, defined by $P_1 \ominus S$.

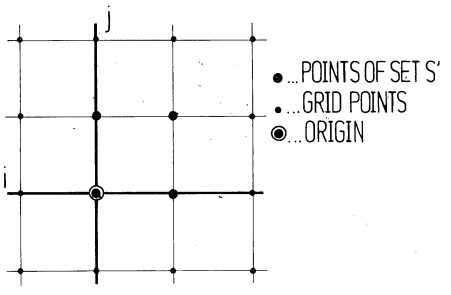

Fig. 7: Set S' to construct the discrete system of Cartesian coordinates.

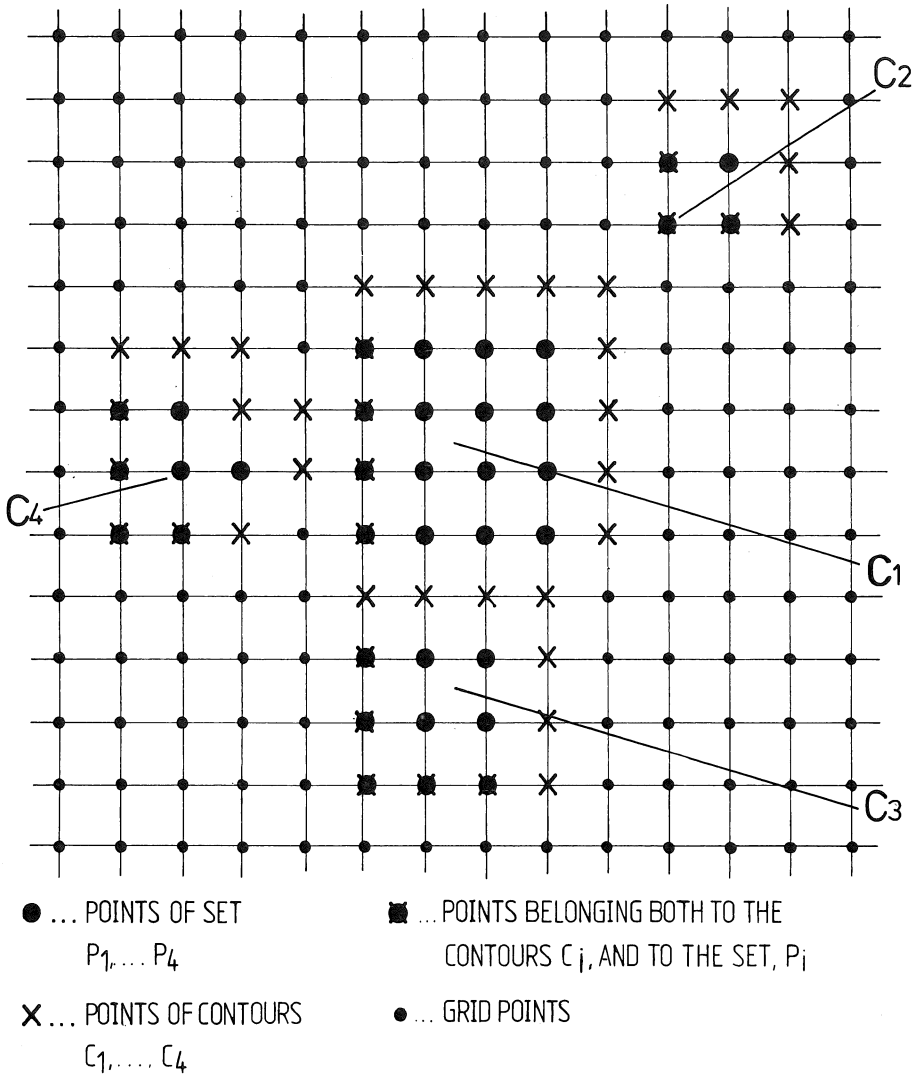

Fig. 8: Sets $P_1,...P_4$ and their contours, $C_1,....C_4$.

3.3 PERFORMING MEASUREMENTS IN HEXAGONAL COORDINATES

The set, S, describing the neighborhood of a point in hexagonal coordinates has the appearance shown in Fig. 9. We can assume that the hexagonal coordinate system was brought about by shearing the system of Cartesian coordinates by 30^{o}. In this case, the Cartesian unit cell, the square, is changed into a rhombus with 60^{o} and 120^{o} angles, respectively. If we shift the unit cells in such a way that one corner each is superimposed upon a grid point, we obtain a contour meeting criteria (14) and (15). However, this violates the neighborhood conditions, because a contour constructed in this way uses points which are not directly adjacent, i.e., which

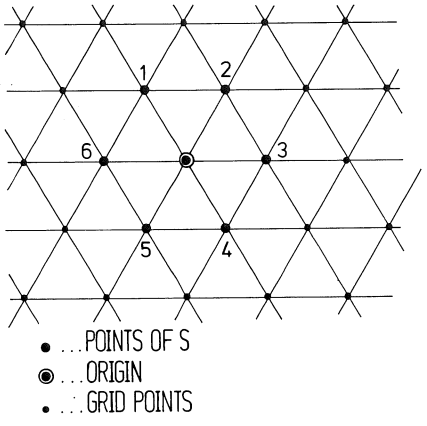

Fig. 9: Set S describing the neighborhood of a point in system of hexagonal coordinates.

is used, besides the origin, are not elements of S. This design of the contour resulting from the distortion of the Cartesian grid consequently cannot be used.

There are only two different possibilities of constructing a contour forming set, S', meeting criterion (9). Besides the origin, these two sets consist either of one point or of two points of S side by side. (One top of this, there are the six sets produced by rotation of S' around the origin). However, it is obvious that the set S' must consist of three points, because if only one point of S no closed contour be produced.

Let us consider the set, S', drawn in Fig. 10, which consists of two points besides the origin. As in the case of the system of Cartesian coordinates, also in the hexagonal case it holds that $S' \oplus \tilde{S}' = S$, if S' is a contour forming set in accordance with (19). If we use the set, S', shown in Fig. 10 to construct a contour in accordance with Eq. (19), we find in calculating the area in accordance with (14) and (16) respectively, that the area calculated in accordance with (16) is always smaller than would correspond to the number of unit cells (Eq. 14). However, since a set consisting of more than three points leads to contours whose intersections do not disappear in accordance with (5), there is no possibility in the hexagonal system to meet all criteria outlined in Section 3.4.1.

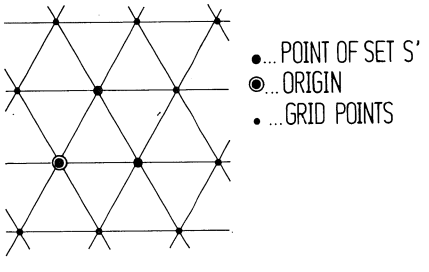

Fig. 10: Set S' to construct the perimeter in a system of hexagonal coordinates.

4. DETERMINING PERIMETERS APPROXIMATING $\mathbb{R}^2$ MEASURES

4.1 CARTESIAN COORDINATES

The dimensions determined by the methods described above are exact quantities. However, in view of the fact that the measurements are carried out in a discrete grid, one obtains the perimeter in the metrics used in $\mathbb{Z}^2$. When further processing the measured results, however, one mostly uses theories and formulae derived for $\mathbb{R}^2$. Consequently, additional coefficients of measure must be determined which approximate the coefficients of measure in $\mathbb{R}^2$. In all approximations one values the connection between two boundary points of the length 1, if it runs parallel to one of the two axes, and with the length $\sqrt{2}$ in those cases in which two adjacent points are connected with each other at the corners. The quality of such approximation for a Euclidean space can be gaged from the quality of the fit of the perimeter of a simple shape to the area described by (14). Measuring, e.g., the area A of a square, one expects a perimeter $P = 4\sqrt{A}$. If the perimeter determined by approximation is P', the quality of the approximation can be described by the relative deviation, Δ:

$$\Delta = \frac{P' - P}{P}$$

The smaller $|\Delta|$, the better the approximation is supposed to be. Gray (1971) offers an interesting solution to this problem of approximation in which four adjacent unit cells (so-called bit quads) are considered. Depending on the number of points of the set to be measured they contain, these bit quads are weighted differently. In the process according to Gray it is necessary to weight differently the points also when measuring an area, depending on the structure of the bit quad containing the point considered. Area measurements according to Eq. (14) are no longer possible in that case. Another drawback of this method lies in the relatively large amount of computer time required to perform such measurements by means of a computer working in the sequential mode. Empirical procedures have shown that good approximations to the perimeter can be obtained by using the following term:

$$P_A = \sum_i I_K(i) + (\sqrt{2} - 1) \sum_i I_{K'}(i) \qquad (21)$$

with the following abbreviations:

$$K' = (K \ominus S_1) \cup (K \ominus S_2)$$

$$K = (B \oplus S'') \cap (\overline{B} \oplus S'')$$

$\ominus$ stands for the Minkowski subtraction.

The set, S'', consists of the origin and the points (1,0) and (0,1) or, correspondingly , of the points obtained when turning S'' by 90° each. The sets, S_1 and S_2, consist of the origin and the points (1,1) and (1,-1), respectively.

Table 2: Measured perimeter and area values of axially parallel squares of different sizes

N	1	2	3	4	5	10
A	1	4	9	16	25	100
P_E	4	8	12	16	20	40
$P_\square$	4	8	12	16	20	40
P_I	1	4	8	12	16	36
Δ_I	-0.75	-0.5	-0.33	-0.25	-0.2	-0.1
A_G	0.5	2.5	6.5	12.5	20.5	90.5
P_{EG}	2.83	6.32	10.2	14.14	18.11	38.04
P_G	2.83	6.83	10.83	14.83	18.83	38.83
Δ_G	0	-0.08	-0.06	-0.05	-0.04	-0.02
P_A	3.41	7.41	11.41	15.41	19.41	39.41
Δ_A	-0.15	-0.07	-0.05	-0.04	-0.03	-0.01

Tables 2 and 3 shown the areas and the perimeters for squares of different sizes, inclined once parallel to the grid and once 45° relative to the grid, as determined by the different methods. To asses the quality of the approximation, the deviation defined in (20) was used. In these tables the following quantities are indicated for squares of different lengths of the edges, N:

- the area, A, according to (14);
- the perimeter, $P_{\square}$, according to (15) (taxi driver metric);
- the "true" perimeter, $P_E = 4\sqrt{A}$;
- the "inner" perimeter, P_i, which is all points of the square having at least one neighboring point in the direction of one axis of the coordinates outside the square (Peipmann, 1976);
- the area, A_G, and the perimeter, P_G, according to Gray, 1971 and the "true" perimeter, P_{EG}, pertaining to the area, A_G;
- the approximate value defined according to (21) of the perimeter, P_A.

Table 3: Measured perimeter and area values of squares of different sizes inclined by 45° relative to the coordinate axes

N	1	2	3	4	5	10
A	1	5	13	25	41	181
P_E	4	8.94	14.42	20	25.61	53.81
$P_{\square}$	4	12	20	28	36	76
P_I	1	4	8	12	16	36
Δ_I	-0.75	-0.55	-0.45	-0.40	-0.38	-0.33
A_G	0.5	4.5	12.5	24.5	40.5	180.5
P_{EG}	2.83	8.49	14.14	19.8	25.46	53.74
P_G	2.83	8.49	14.14	19.8	25.46	53.74
Δ_G	0	0	0	0	0	0
P_A	3.41	9.07	14.73	20.38	26.04	53.33
Δ_A	-0.15	-0.01	0.02	0.02	0.02	0.01

Let us first of all consider the values shown in Table 1 for the perimeter of axially parallel squares and their deviations from the Euclidean "true" perimeter; in this case, the approximate values calculated in accordance with Eq. (21) shown the most favorable result. In the squares turned 45°, conditions look slightly different. In the shapes one obtains an error of zero when using Gray's formulae, while the use of (21) produces errors in the range between one and two percent. It is seen that the relatively sophisticated way in which Gray measures the area produces only slight advantages for the two shapes considered. The disadvantage of greater computing expenditure probably weighs more heavily. The "inner" perimeter in all cases deviates very much from the true perimeter. For large values of N, all approximated values for the perimeter converge towards the true perimeter, thus rendering these considerations invalid for sufficiently large squares. In general, however, it is not the areas and perimeters of squares which must be determined, but those of random shapes. Such shapes in principle can be described by a series of small squares of the two types described above. Consequently, it is important also when dealing with small basic patterns to obtain the best possible approximations to the perimeter.

Exact results can be expected only in the absence of the approximations to the Euclidean space and if the measured values are determined and processed under the conditions of taxi metrics in $\mathbb{Z}^2$.

4.2 HEXAGONAL COORDINATES

Unlike Cartesian coordinates, in hexagonal coordinates, the distance between two adjacent points is always unity. This facilitates determining coefficients of measure for the perimeter, which are approximated to the values of $\mathbb{R}^2$. Gray (1971) indicates a formula for the perimeter based on counting the six possible groups of two unit cells, each containing the values 0 and 1. The area used by Gray in this case is the number of points. Another approximation is obtained by determining the perimeter analogously to the Cartesian system (Eq. 21). In the present hexagonal system, this leads to the formula

$$P_A = \sum_1 I_K \quad (1) \qquad (22)$$

with the abbreviation

$$K = (B \oplus S'') \cap (\overline{B} \oplus S'')$$

Table 4: Areas and perimeters of hexagons of various sizes determined by different methods

N	1	2	3	4	5	10
A	1	7	19	37	61	271
A_I	0.5	6.5	18.5	36.5	60.5	270.5
P_E	3.46	9.17	15.1	21.07	27.6	53.03
P_I	1	6	12	18	24	54
Δ_I	-0.71	-0.35	-0.21	-0.15	-0.11	-0.05
P_G	3.46	10.04	17.3	24.2	31.2	65.8
Δ_G	0	0.1	0.01	0.01	0.01	0.02
P_A	3	9	15	12	27	57
Δ_A	-0.13	-0.02	-0.01	-0.003	-0.002	-0.001

The set, $S'' \subset S$, consists of the origin and two adjacent points side by side. To shown the quality of these approximations, the values measured for the perimeter by the different techniques are summarized in Tables 4 and 5 for hexagons and triangles, respectively, of different sizes and the deviations defined according to (20) are entered. The following quantities are shown in Tables 4 and 5:

- the lengths of the edges of the hexagon and the triangle, respectively;

- the area, A, of the shapes, which is obtained by counting the unit cells occupied (Eq. 14);

- the area, A_I, according to Eq. 16. This quantity was entered in order to indicate errors between an area measurement by counting points and by planimetry in a hexagonal system of coordinates;

- the "true" perimeter, P_E, of the shapes in $\mathbb{R}^2$;
- the inner perimeter, P_i, which is the number of points of the shapes having at least one neighbor outside the shape;
- the perimeter, P_G, according to Gray (1971);
- the approximate value defined according to (22) of the perimeter, P_A, in $\mathbb{R}^2$.

Table 5: Areas and perimeters of equilateral triangles of different sizes determined by different techniques

N	2	3	4	5	10
A	3	6	10	15	55
A_I	2	4.5	8	12.5	50
P_E	7.35	10.39	13.42	16.43	31.46
P_I	3	6	9	12	27
Δ_I	-0.59	-0.42	-0.33	-0.27	-0.14
P_G	6.9	10.4	13.9	17.3	34.6
Δ_G	-0.1	0.001	0.04	0.05	0.14
P_A	6	9	12	15	30
Δ_A	-0.18	-0.13	-0.12	-0.09	-0.05

As in the case of Cartesian coordinates, also in the hexagonal system the difference between the "true" perimeter and the different approximations converges towards zero as the shapes increase in size.

As in the case of Cartesian coordinates, the deviation is a maximum for the inner perimeter. Clearly the smallest deviations are shown by the approximate value of the perimeter defined according to Eq. (22).

Although, in hexagonal coordinates, there is no ident-

ity between the area as determined by counting points and that determined by tracing contours (planimetry), the approximations obtained for the perimeter in $\mathbb{R}^2$ are roughly as good as those in the Cartesian system.

5. DETERMINING THE EULER NUMBER (PARTICLE NUMBER)

In addition to the area and the perimeter of the subsets, G_i, of an image, B, frequently also the number of unconnected subsets, G_i, within B is of interest. Besides, it is of interest to see whether the subsets, G_i, have simple or multiple connectivities. If N particles, G_i, are contained within B, which have a total of L holes, the Euler number, E, of B in a two-dimensional space is

$$E = N - L.$$

For a single particle, the number of holes is equal to its connectivity, which is the number of sections by which a particle can be cut without increasing the number of particles (De Hoff, 1968).

According to Gray (1971), the Euler number can be determined by counting the "critical points." If we look at the conditions in $\mathbb{R}^2$, these critical points, P_1 and P_2, are determined with respect to a tangent vector, $\vec{t}$. One counts all points, P_1, of the contour of a particle (or the contours of all particles in B) having the tangent vector, $\vec{t}$, and a positive curvature and all points, P_2, with the same tangent vector and a negative curvature. The Euler number, E, then is obtained from

$$E = P_1 - P_2.$$

If it is not the Euler number but the number of particles in B, which is to be determined, the holes in the particles must be closed before beginning the measurement. In special cases it is possible to separate before the measurement connected particles to be counted separately.

5.1 DETERMINING THE EULER NUMBER IN CARTESIAN COORDINATES

The Euler number can be found either by determining the local properties of the individual particles (Gray, 1971) or by erosion and dilatation by means of appropriately selected structural elements.

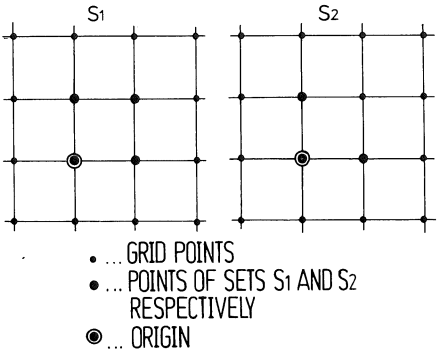

Fig. 11: Sets S_1 and S_2 determining the Euler number in Cartesian coordinates.

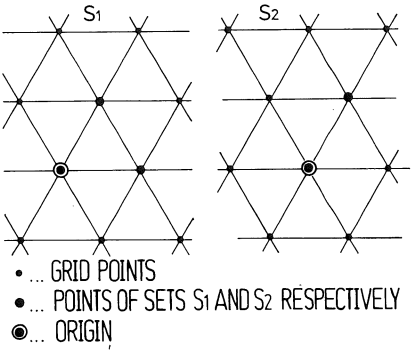

Fig. 12: Sets S_1 and S_2 determining the Euler number in hexagonal coordinates.

If the Euler number is to be determined by way of the local characteristics, e.g., all bit quads with the structure of $\begin{bmatrix} 00 \\ 10 \end{bmatrix}$ are counted and in this way the number, P_1, of critical points with positive curvatures is determined. The number, P_2, of the points with negative curvatures is obtained by counting the bit quads with the structure of $\begin{bmatrix} 10 \\ 11 \end{bmatrix}$ and $\begin{bmatrix} 10 \\ 01 \end{bmatrix}$ (Gray, 1971). If the Euler number is to be determined by Minkowski additions and subtractions, it is obteined from

$$P_1 = A\,(B \oplus S_1) - A\,(B \oplus S_2)$$

$$P_2 = A\,(B \ominus S_3) - A\,(B \ominus S_1) - A\,(B \ominus \tilde{S}_2)$$

$$E = P_1 - P_2$$

It is seen that this method allows the determination of the Euler number to be reduced to five area measurements in accordance with (15). The sets, S_1 and S_2, are drawn in Fig. 11. S_3 consists of the points (0,0) and (-1,1).

5.2 DETERMINING THE EULER NUMBER IN HEXAGONAL COORDINATES

As in Cartesian coordiantes, also in hexagonal coordinates the Euler number can be determined by local operations or by area measurements. In hexagonal coordinates, the number of critical points with positive curvatures is equal to the bit triads of the type of $\begin{bmatrix} 00 \\ 1 \end{bmatrix}$. The number of points, P_2, is obtained by counting the bit triads with the structure of $\begin{bmatrix} 0 \\ 11 \end{bmatrix}$ (Gray, 1971 , Hersant, Jeulin, Paniere, 1975).

In a way completely analogous to the conditions in Cartesian coordinates, also in a hexagonal coordinate system the Euler number can be determined by four area measurements. The sets, S_1 and S_2, by means of which the original image must be transformed prior to the measurement, is shown in Fig. 12.

5.3 DETERMINING PARTICLE NUMBERS

If it is not the Euler number but the number of particles, which is to be determined, basically the same techniques are applied as are used to determine the Euler number. However, the holes in the particles must be closed before the measurements. Two methods can be applied to close the holes in the particles. In each case it must be examined which of the two methods is most advantageous, i.e., can be applied with a minimum of computer time.

Initially, it can be assumed that an image, B, is decomposed into subimages, B_1, by means of masks, F_1.

$$B_1 = B \cap F_1 \qquad 1 \in \{1, \ldots, L\}$$

Closing the holes is achieved by Minkowski additions of sets, E_i, consisting of one each of the eight individual points adjacent to the origin and the origin proper, to the complement of the mask and by the connection of this changed mask to the subimage, B_1:

$$\overline{F_1}\,(k) = \bigcup_{i=1}^{8} \left(F_1\,(k-1) \oplus E_i \right) \cap \overline{B_1} \qquad 1 \in L,\ k \in \mathbb{N}$$

If the changed mask, $F_1\,(k)$, is equal to the mask, $F_1\,(k-1)$, from the previous step in iteration, it holds that

$$F_1\,(k) = B'_1$$

where B_1' is equal to the image, B_1, in which the holes in the particles are closed. The mask, $F_1\,(0)$, is identical with the measuring mask, F_1.

The other possibility of closing holes is by dilatation of the individual particles ob $\overline{B}$ with the sets E_i described above, followed by a reconstruction step. This process must be repeated iteratively until the image does not change any more:

$$B'(k) = \bigcup_{i=1}^{8} \left[B'(k-1) \oplus E_i \right] \cap \overline{B} \qquad k \in \mathbb{N}$$

If $B'(k) = B'(k-1)$, then $B'(k) = B'$, the image B in which the holes within the particles are closed. This iteration begins at $B'(0) = B$.

In special cases it is also possible to separate connected particles for separate counting. Meyer, (1979) has indicated an algorithm for this purpose.

6. CONCLUSIONS

It has been shown in this study how to extract measured values from an image. The basis used thoughout was a description of the image and of its elements by means of the methods of the theory of sets. A major complication arises from the fact that the image is not evaluated in a continuous Euclidean, one must in a discrete space. As in any digitization, one must realize also in this case that the transition from a continuous to a discrete space entails the characteristic errors. These errors must be recognized and precautions must be taken to prevent their producing inconsistent results or results contradicting observations. A characteristic example is the measurement of perimeters. To allow uniform processing of the images on a computer, formulae have been indicated for all coefficients of measure to reduce these to operations using sets and to area measurements.

In all chapters of this study a comparison is made between Cartesian and hexagonal tessellation of the plane. In designing a new image processing system, such as the PACOS system (Vollath, 1982), a decision must be taken in favor of one of the two systems. The PACOS image processing system uses Cartesian coordinates. Although the advantages of the Cartesian system over the hexagonal system are not very significant at the level of fundamental considerations, they do become apparent in considering the necessary detailed algorithms which, however, have not been discussed in this study. Another major item not discussed in this paper is the correction of the error caused by the rim of the mask. This part was left out because it is related mainly to the evaluation of the readings, not to surveying the image proper.

REFERENCES

Coxeter, H.S.N., Unvergängliche Geometrie, Birkhäuser Verlag Basel, Stuttgart, 1963: p. 86-90.

De Hoff, R.T., Quantitative Microscopy, Edt. R.T. De Hoff, F.N. Rhines, Mc Graw-Hill Book Comp., 1968: 291-325.

Gray, S.B., Local Properties of Binary Images in Two Dimensions, IEEE Trans. on Comp. C-20, 1971: 551-561.

Hadwiger, H., Minkowskische Addition und Subtraktion beliebiger Punktmengen und die Theoreme von Erhard Schmidt, Mathem. Zeitschrift 53, 1950: 210-218.

Hersant, T., Jeulin, D., Parniere P., Basic Notions of Mathematical Morphology used in Quantitative Metallography, IRSID-Report, RE 322 bis Par. 1, 1975.

Matheron, G., Eléments pur une Théorie des Milieux Poreau, Masson, Paris, 1967.

Meschkowski, H., Theorie der Punktmengen, BI-Wissenschaftsverlag, Mannheim, 1974.

Meyer, F., in Nawrath, R., Serra, J., Quantitative image analysis: Applications using sequential transformations, Microscopica Acta 82, 1979: 113-128.

Peipmann, R., Erkennen von Strukturen und Mustern, Walter de Gruyter Berlin, New York, 1976: p. 219.

Rosenfeld, A., Pfaltz, J.L., Sequential Operations in Digital Picture Processing, JACM 13, 1966: 471-494.

Rosenfeld, A., Pfaltz, J.L., Distance Functions on Digital Picture, Pattern Recognition 1, 1968: 33-61.

Rosenfeld, A., Connectivity in Digital Pictures, JACM 17, 1970: 146-160.

Vollath, D., The Image Analysing System PACOS, Part. 1 Construction and Method of Operation, The Image Analysing System PACOS, Part. 2 Examples of Application, Praktische Metallographie 19, 1982: 7-23, 94-103.

Received: 1984-06-29
Accepted: 1984-10-25